Electronic structure of $BaSn_{1-x}Sb_xO_3$ studied by photoemission spectroscopy

R. Claessen
Randall Laboratory, University of Michigan, Ann Arbor, Michigan 48109-1120

M. G. Smith and J. B. Goodenough
Center for Materials Science & Engineering, ETC 5.160, The University of Texas at Austin, Austin, Texas 78712-1084

J. W. Allen
Randall Laboratory, University of Michigan, Ann Arbor, Michigan 48109-1120

(Received 6 July 1992; revised manuscript received 27 August 1992)

We have studied the electronic structure of $BaSn_{1-x}Sb_xO_3$ by photoemission and bremsstrahlung isochromat spectroscopy. The Sb 3*d* core-level spectra show the presence of only Sb^{5+} ions and give no evidence for charge disproportionation into Sb^{3+} and Sb^{5+}. The combined valence- and conduction-band spectra are found to be in good agreement with band theory and indicate that, upon doping, the Fermi level is placed at the bottom of the conduction band. We discuss the spectroscopic results in relation to earlier Mössbauer and transport data and propose a model of the electronic structure in which the electrons introduced by the Sb doping occupy the lowest-lying Sn-5*s*–derived conduction-band states. This scenario can be obtained by a static oxygen displacement, which would stabilize the Sb^{5+} valence state by lifting the Sb 5*s* states well above the conduction-band minimum.

I. INTRODUCTION

Recently the system $BaSn_{1-x}Sb_xO_3$ has aroused some interest as the 5*s*-orbital analog to the family of the cubic perovskites based on $BaBiO_3$ and $BaPbO_3$. While a number of the 6*s* systems display superconductivity with critical temperatures of up to 30 K [for $Ba_{0.6}K_{0.4}BiO_3$ (Ref. 1)], no superconducting behavior has been observed in $BaSn_{1-x}Sb_xO_3$ down to 0.05 K and for antimony concentrations up to the solubility limit of $x \approx 0.2$.[2] Moreover, in contrast to the metallicity of $BaPbO_3$,[3] undoped $BaSnO_3$ is an insulator with a band gap of 3.4 eV (Ref. 4) between the mostly O 2*p*-derived valence band and the antibonding (σ^*) conduction band consisting dominantly of Sn 5*s* orbitals with some O 2*p* admixture.[5] Upon doping with Sb in the range $0 \leq x \leq 0.15$ the resistivity decreases with increasing x and appears to be virtually independent of temperature from 4.2 to 300 K.[2] In order to explain their resistivity data, Cava *et al.*[2] suggested a model in which most of the doped electrons are trapped due to microscopic Sb^{3+}-Sb^{5+} or Sn^{2+}-Sn^{4+} charge disproportionation while the few remaining carriers travel in a narrow impuritylike midgap band. However, recent Mössbauer studies on the valence states of Sn and Sb found no evidence for charge disproportionation.[6,7]

In this paper, we report on photoemission measurements on $BaSn_{1-x}Sb_xO_3$ ceramic samples. From x-ray-photoemission spectroscopy (XPS) on the core levels, we find no evidence for charge disproportionation on the Sb atoms, but only 3*d* binding energies characteristic of the 5+ valence state. Combined ultraviolet photoemission (UPS) and bremsstrahlung isochromat spectroscopy (BIS) on the valence and conduction bands, respectively, suggest that the Fermi energy is located at or very close to the conduction-band minimum. No evidence is found for the existence of a conducting, narrow impurity band in the insulator gap. By taking into account recent data on the Seebeck effect,[6] we propose a model for the electronic structure in which the low-lying Sn 5*s*-derived (σ^*) states become occupied upon doping and are responsible for the conductivity. We discuss a mechanism that could explain the stabilization of the Sb^{5+} valence state leading to the above picture.

II. EXPERIMENTAL DETAILS

Ceramic samples of $BaSn_{1-x}Sb_xO_3$ were prepared by solid-state reaction. Stochiometric amounts of $BaCO_3$, SnO_2, and Sb_2O_3 were mixed in a mortar and pestle and fired at 1200 °C for 16 h. The resulting powders were reground and pressed into pellets. The undoped $BaSnO_3$ sample was annealed in air at 1300 °C for 43 h and slowly cooled to room temperature. For $x = 0.1$ and 0.15, $BaSn_{1-x}Sb_xO_3$ was annealed in air at 1500 °C for 65 h with two intermediate grindings and pressings into pellets. In order to study the effect of oxygen reduction, $BaSn_{1-x}Sb_xO_{3-\delta}$ was prepared in flowing N_2 at 950 °C for 12 h with slow cooling to room temperature. The products were all single phase, as found by x-ray powder diffraction recorded with Cu $K\alpha$ radiation.

Experimental spectra were measured in a VG ESCALAB, using the He I ($h\nu = 21.22$ eV) and He II (40.82 eV) lines for UPS and monochromatized Mg $K\alpha$ (1486.6 eV) radiation for XPS. The BIS spectrometer utilizes the same x-ray monochromator as the XPS system and, therefore, operates at the same photon energy. The energy resolutions used here are 0.05, 1.1, and 0.65 eV (full width at half maximum) for UPS, XPS, and BIS, respectively. As a reference point for the binding energies, we used the Fermi edge of a clean silver sample measured

under identical conditions. All experiments were performed at a base pressure of 5×10^{-11} Torr. Clean surfaces of the ceramic samples were prepared by scraping with a diamond file until the XPS spectra were found to be free of signals due to carbon or other contaminants. In order to suppress diffusion of contaminants along the grain boundaries, the samples were kept cooled at a temperature of about 100 K.

III. RESULTS

All samples were checked for their chemical purity by performing XPS over a broad range of binding energies. Except for an emission from the carbon 1*s* core level on *as-grown* samples, no foreign elements were found. Carbon is a typical surface contaminant, essentially residing as CO on the grain boundaries, and could be easily removed by scraping with a diamond file. We used the areas under the Sn and Sb 3*d* core-level emissions to obtain a rough measure of the surface stoichiometry. Table I shows the surface-atomic ratios obtained from the XPS data by taking into account the respective photoionization cross sections.[8] The result indicates that there is more Sb at the surface than might be expected from the nominal bulk composition. A similar observation has been reported earlier[4] and attributed to small amounts of impurity phases such as Sb_2O_5, presumably concentrated at the grain boundaries. Note that their volume fraction must be small, since they were not detectable by x-ray diffraction. However, it is also possible that at least part of the observed Sb excess is an artifact introduced by the surface preparation. Scraping disrupts the surface, and the ion with the lowest surface energy can be expected to migrate preferentially to the surface. In vacuum, an oxygen deficiency at the surface can be expected to stabilize preferentially in the lower oxygen coordination of the smaller Sb^{5+} ion with its stronger covalent bonding. This may affect the UPS data even more due to the slightly enhanced surface sensitivity compared to XPS.

Figure 1 shows an XPS spectrum of $BaSn_{0.85}Sb_{0.15}O_3$ covering the Sb 3*d* and O 1*s* core-level emissions. The peak at 540.1-eV binding energy corresponds to the Sb $3d_{3/2}$ level, while the Sb $3d_{5/2}$ and O 1*s* levels overlap to give rise to the intense peak at 530.5 eV. We constructed the Sb $3d_{5/2}$ emission from the $3d_{3/2}$ peak using the known spin-orbit splitting[9] and intensity ratio. This allowed us to decompose the large peak into the Sb $3d_{5/2}$ and O 1*s* contributions, shown in Fig. 1 as solid and dashed curves, respectively. From this we obtain an O 1*s* binding energy of 530.3 eV, which was reproducible for all samples. The O 1*s* line shape in Fig. 1 is quite symmetric with no apparent side structure, which (within the limitations of the decomposition procedure) indicates a clean and homogeneous surface.

TABLE I. Measured and expected Sb-to-Sn surface-atomic ratios of $BaSn_{1-x}Sb_xO_3$. The experimental values have been determined from XPS intensities of the $3d_{3/2}$ core levels, taking into account the element specific photoionization cross sections.

Sample	Sb/Sn (theor.)	Sb/Sn (meas.)
$x=0$	0	0
$x=0.10$	0.11	0.17
$x=0.10$ (reduced)	0.11	0.18
$x=0.15$	0.18	0.24

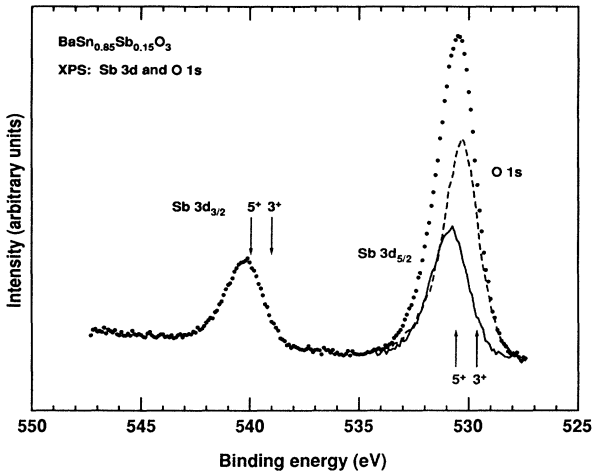

FIG. 1. XPS spectrum of $BaSn_{0.85}Sb_{0.15}O_3$ showing the Sb 3*d* and O 1*s* core levels. The solid and dashed curves show the decomposition of the large peak at 530.5 eV into the Sb $3d_{5/2}$ and O 1*s* core-level emissions. The Sb $3d_{5/2}$ peak has been constructed from the Sb $3d_{3/2}$ peak using the known spin-orbit splitting and intensity ratio. The arrows denote the binding energies of the Sb 3*d* emissions for trivalent and pentavalent antimony.

The arrows in Fig. 1 indicate the energy positions of the Sb 3*d* emissions for trivalent and pentavalent antimony as they are found in Sb_2O_3 and Sb_2O_5, respectively.[9] The chemical shift between these two valence states is about 1 eV. Clearly, the binding energies measured for $BaSn_{0.85}Sb_{0.15}O_3$ are consistent with a 5+ valence state. A substantial contribution from Sb^{3+}, as predicted in the charge disproportionation model, would give rise to a characteristic double-peak structure or at least a strong asymmetry of the Sb $3d_{3/2}$ core-level emission. Within the experimental accuracy, the Sb $3d_{3/2}$ emission consists of a single line and shows no evidence for the existence of Sb^{3+} ions. This result was obtained for all Sb-doped samples. Concerning the valency of the Sn atoms, we cannot derive any conclusions from the XPS data because the Sn core levels do not display a detectable chemical shift between the 2+ and 4+ valence states.[9]

We now turn to the UPS results on the valence-band structure. In Fig. 2, we show the valence-band spectra for the sample with $x=0.15$ and two samples with $x=0.10$, one of which had been reduced in nitrogen atmosphere. Except for an overall shift of ~0.2 eV of the $x=0.10$ spectra to higher binding energy, there seem to be no significant differences in the spectra. The valence-band edges as obtained from extrapolating linearly from the point of steepest descent in the valence-band onset down to the baseline are located 2.8 and 3.0 eV below the Fermi level E_F for $x=0.15$ and 0.10, respectively. These values have to be compared to the band gap of 3.4 eV in

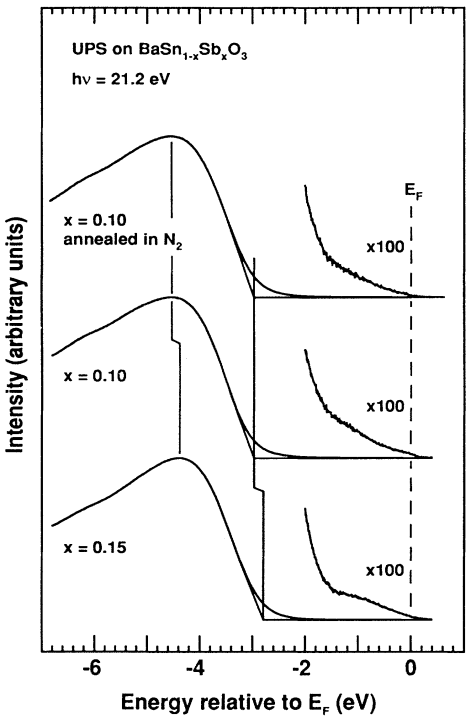

FIG. 2. Valence spectra of samples with different doping levels and heat treatments. The near-E_F emission is shown on a greatly enlarged intensity scale. Note that the spectra have been corrected for He I satellite radiation.

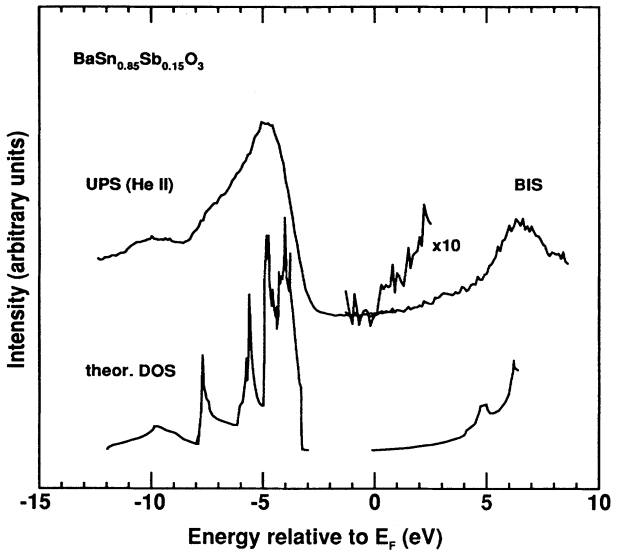

FIG. 3. Valence- and conduction-band spectra of $BaSn_{0.85}Sb_{0.15}O_3$ measured by UPS ($h\nu$=40.8 eV) and BIS, respectively. Also shown is the band-structure calculation of Singh *et al.* (Ref. 5) for undoped $BaSnO_3$, adjusted to the experimentally determined band gap (see text).

undoped $BaSnO_3$, as has been determined by reflectivity measurements.[4,10] Thus we find the chemical potential near or at the top of the insulator gap, which additionally seems to become somewhat reduced upon doping. If the Fermi level is indeed located at the bottom of the conduction band, we would expect to observe the low-lying conduction-band states and to see a metallic Fermi edge. However, this does not seem to be the case. In Fig. 2, we also show the near-E_F part of the valence-band spectra on a greatly enlarged intensity scale. Note that the spectra have been numerically corrected for the He I_β and He I_γ radiation satellites in order to exclude artificial structures. We find a small emission between the Fermi level and 1.5-eV binding energy; it continuously decreases on going toward E_F with no apparent Fermi-Dirac cutoff. In both intensity and structure this feature does not seem to depend significantly on doping or reduction treatment. Therefore we conclude that it is not intrinsic to $BaSn_{1-x}Sb_xO_3$, but is probably due to defect states on the surface and/or the grain boundaries.

Figure 3 shows a BIS spectrum of the conduction band of $BaSn_{0.85}Sb_{0.15}O_3$ in combination with a He II valence-band spectrum and in comparison to a band-structure calculation, which will be discussed in the next section. Though the statistical noise in the BIS data does not allow us to identify a Fermi edge, there is a slowly decreasing but finite emission for all energies down to the Fermi energy. Thus, from the combined UPS and BIS spectra we may conclude that the chemical potential is located at or very close to the conduction-band minimum, which is poorly defined because of the "tailing" of the band edges.

IV. DISCUSSION

Our XPS data on the binding energy and the line shape of the Sb 3*d* core level identify the antimony valence as 5+ with no evidence for a charge disproportionation into Sb^{3+} and Sb^{5+}. This confirms the results of Mössbauer spectroscopy,[6,7] in which the isomer shift for Sb lies well within the range for Sb^{5+} in other oxides. While XPS can yield no information on the valence state of tin, the Mössbauer data show a single line with an isomer shift corresponding to a valence of $(4-\delta)+$, where δ indicates a small amount of extra charge on the Sn sites.[6]

Cava *et al.*[2] were led to propose charge disproportionation by their finding that an estimate of the minimum conductivity, assuming one carrier for every Sb atom and a mean free path of the order of the lattice constant, is still by a factor of 20 larger than the measured conductivity. They argued that this discrepancy could be accounted for by trapping most of the free carriers by charge disproportionation on the Sb or Sn atoms. However, both the XPS and the Mössbauer results are incompatible with a charge disproportionation which could lead to a trapping of at least 95% of the carriers, as required in this picture. We can only speculate about the cause of the discrepancy between the measured and estimated conductivity, but we may note here that the resistivity measurements of Ref. 2 were performed on ceramic samples in which transport across grain boundaries could dominate the resistivity.

In Fig. 3, we compare the combined UPS/BIS spectra of $BaSn_{0.85}Sb_{0.15}O_3$ to a density-functional calculation of the electronic structure of undoped $BaSnO_3$.[5] It is a well-

known problem of density-functional theory to underestimate considerably the gap between the valence and the conduction bands. We have therefore deliberately positioned the theoretical bands such that the experimental value of 3.4 eV (Ref. 4) for the insulator gap is reproduced and that the chemical potential lies at the conduction-band minimum (CBM). The similarity between the calculated and measured electronic structure is striking. The valence-band feature at 10-eV binding energy can be identified with the Sn $5s$–O $2p$ bonding σ band. The corresponding antibonding σ^* band of essentially Sn $5s$ nature constitutes the conduction band. The bulk of the valence-band emission between -8 eV and the valence-band maximum is due to bonding π bonds of O $2p$ parentage. The prominent feature in the BIS spectrum at 6 eV above the Fermi level is attributed to Ba $6s$ states.

The fact that we seem to be unable to observe a finite density of states at E_F and a clear Fermi edge by photoemission may be accounted for by the extremely small density of states at the CBM predicted by the band theory (cf. Fig. 3). A simple estimate assuming that the doped electrons reside in the CBM and additionally accounting for the UPS photoionization cross sections of the conduction (Sn $5s$) and valence (mostly O $2p$) band states[8] yields, for a doping level of $x=0.15$, a spectral weight of $<5\times10^{-4}$ for the occupied conduction-band states relative to the strength of the valence-band emission. This would hardly be visible even on the enlarged intensity scale of Fig. 2, and may be therefore beyond the detection limit.

But even without a direct observation of a Fermi edge, the combined UPS/BIS results indicate that the Fermi energy is located at or at least very close to the CBM. In principle, the UPS data do not allow us to decide whether the Fermi level is slightly above the CBM, i.e., with the lowest-lying σ^* states being occupied, or whether the Fermi level is pinned by very shallow donor levels just below the CBM. However, there is other experimental evidence that favors the picture of a slightly filled conduction band. Measurements of the Seebeck coefficient show a negative sign and a linear temperature dependence[6] typical for degenerate electronic conduction in a band of itinerant electronic states. Also, the slight deviation of the Mössbauer isomer shift in Sn from a value corresponding to Sn^{4+} is consistent with a valence of $3.82+$ expected for a situation where the extra electrons introduced by an $x=0.15$ Sb doping go into unoccupied Sn $5s$ orbitals.[6] Furthermore, the Mössbauer data show no temperature dependence of the Sn valence between 1.2 and 300 K. If there were shallow donor levels below the CBM, their activation energy would be considerably smaller than 1.2 K. In this case, we would obtain a picture of a highly degenerate semiconductor for temperatures above ~1 K, and for all practical purposes there would be no difference from a metallic ground state. Differences between the two scenarios would only become apparent well below 1 K.

These findings seem to be surprising in light of the fact that the atomic binding energy of the Sb $5s$ orbital is larger than that of Sn $5s$.[2] We illustrate this in a schematic molecular orbital (MO) picture in Fig. 4. In the undoped insulator, the hybridization between Sn $5s$ and O $2p$ orbitals leads to occupied bonding σ and π states and the antibonding σ^* conduction-band states. If we now replace Sn by Sb with its larger $5s$ binding energy, and assume the same $5s$-$2p$ hybridization energy as for Sn, the corresponding $sp\sigma^*$ hybrid will lie in the insulator gap, i.e., *below* the corresponding Sn $sp\sigma^*$ states. This is why Cava *et al.*[2] suggested the existence of a narrow impuritylike midgap band of Sb $5s$ parentage that is partially filled and in which the untrapped fraction of the carriers travel. However, as shown above, this scenario is incompatible with the spectroscopic evidence.

A mechanism that would explain the filling of unoccupied Sn $5s$ rather than Sb $5s$ states and the stabilization of the Sb^{5+} valence state has been suggested earlier by some of us.[6] The perovskite structure of $BaSnO_3$ contains a 180° Sn-O-Sn link that is symmetric about the oxygen site. Upon replacing one of the Sn atoms by Sb, the symmetry is broken, and there is no reason why the original bond lengths and the $5s$-$2p$ hybridizations should be preserved. In fact, from the known Sb-O and Sn-O equilibrium bond lengths, a static displacement of the oxygen toward the Sb atom can be expected. Octahedrally coordinated Sb^{5+} in Sb_2O_5 has a shortest Sb-O bond of 1.91 Å and a longest of 2.08 Å.[11] An increase with x in the room-temperature lattice parameter of $BaSn_{1-x}Sb_xO_3$ is consistent with the addition of one electron per Sb to the antibonding σ^* band. A room-temperature lattice parameter for $x=0.15$ of 4.11 Å and an equilibrium Sn-O bond length, from ionic radii, that is >2.09 Å (in the

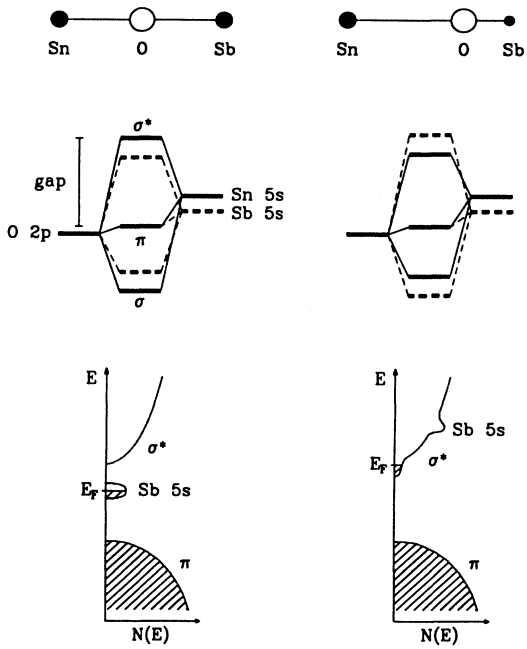

FIG. 4. Top row: schematic energy-level diagram in a molecular orbital (MO) picture for a situation with the oxygen atom at the center of the 180° Sn-O-Sb link (left) and with the oxygen displaced toward the Sb (right); bottom: the same for a bandlike density-of-states picture. See the text for a discussion.

presence of σ^* electrons) gives a Sb-O length <2.02 Å, which is compatible with a shortest Sb-O length of 1.91 Å for Sb^{5+}.

If we assume that the oxygen is statically displaced toward the Sb atom, we obtain the situation shown on the right side of Fig. 4. The Sb $5s-O\,2p$ hybridization is now increased, whereas the local Sn-O bond length becomes larger and the corresponding hybridization smaller. Thus, the energies of the Sb- and Sn-derived σ^* states are reversed in order, with the bottom of the Sn $5s-O\,2p$ antibonding band becoming lower than the Sb $5s$ states. In this picture there is no midgap impurity band, and the doped electrons populate the lowest-lying Sn $sp\sigma^*$ conduction-band states in complete accordance with the combined photoemission, BIS, and Mössbauer data. Since not all Sn $5s-O\,2p$ σ^* states will be lowered in energy, but only those in the local vicinity of a Sb atom, the number of states at the CBM will be proportional to the Sb concentration x and therefore even smaller than the already very low density of states expected for the undistorted crystal structure, contributing to our difficulty of observing a Fermi edge in the photoemission spectra. Also, the slight energy lowering of the Sn $sp\sigma^*$ band with respect to the O $2p_\pi$ bands, which are expected to be largely insensitive to the doping, could explain the reduced gaps between valence and conduction bands (2.8 eV for $x=0.15$ and 3.0 eV for $x=0.10$) determined for the doped samples as compared to the 3.4-eV insulator gap[4] in $BaSnO_3$. (However, we should mention here that the electrolyte electroreflectance measurements in Ref. 4 found the gap to be independent of doping up to $x=0.10$ and to increase slightly above that level.) The bottom of Fig. 4 shows how the MO picture translates into a band structure. The additional occupied Sb $sp\sigma$ and unoccupied Sb $sp\sigma^*$ states suggested in Fig. 4 may not be visible in UPS and BIS, respectively, at the small Sb concentrations used here. In order to test this model and to obtain information on a possible displacement of oxygen atoms, extended x-ray-absorption fine-structure (EXAFS) measurements are in progress.

The picture of the electronic structure described above is able to explain the observed transport properties at least on a qualitative level. With the lowest-lying σ^* conduction-band states occupied, we have itinerant n-type carriers as suggested by the results on the Seebeck coefficient.[6] At the Sb-doping levels considered here, impurity scattering will dominate the dissipation of electrical current, thus accounting for the temperature independence of the resistivity.[2] As the Sb concentration becomes bigger, the resistivity is found to decrease,[2] because the increase in the density of carriers doped into the conduction band is more important than the reduction of the mean free path. Concerning the absence of superconductivity, structural details such as the proposed static displacement of oxygen atoms will certainly be of importance. However, our spectroscopic result that the density of states at the Fermi level, $N(E_F)$, is extremely small already indicates that a critical temperature would be very low in any case.

As far as a quantitative understanding of the properties of $BaSn_{1-x}Sb_xO_3$ is concerned, a number of problems remain, such as the above-mentioned discrepancy between the resistivity measured by Cava *et al.* and an estimate of the minimum conductivity.[2] We speculated that their result may have been dominated by transport across grain boundaries. In our photoemission spectra of ceramic samples we also saw effects due to the existence of grain boundaries, and we have no way of quantitatively determining the fraction of the surface consisting of grain boundaries. Therefore, further transport and photoemission studies on *single-crystalline* material are highly desirable.

V. CONCLUSION

In summary, we have studied the electronic structure of $BaSn_{1-x}Sb_xO_3$ by photoemission and BIS. The Sb $3d$ core levels show the presence of only Sb^{5+} ions and yield no indication for the existence of charge disproportion on antimony. The combined UPS/BIS spectra are in very good agreement with a band-structure calculation and show that in the doped samples the Fermi level lies at the bottom of the antibonding conduction band, though we cannot directly observe a Fermi edge. We find no evidence for an Sb $5s$–derived midgap impurity band. Based on the photoemission results, and taking into account earlier Mössbauer and Seebeck data, we obtain a picture of the electronic structure in which the electrons introduced by the Sb doping go into the low-lying Sn $5s$–derived conduction-band states while the corresponding Sb $5s$ states are higher in energy and remain thus unoccupied. A static displacement of oxygen atoms toward the Sb impurities is a possible mechanism that could stabilize the Sb^{5+} valence state and lead to this scenario.

ACKNOWLEDGMENTS

One of us (R.C.) gratefully acknowledges support by the Alexander von Humboldt Foundation, Bonn, Germany. The work at the University of Michigan was supported by NSF Grant No. DMR-91-08015. The work at the University of Texas was supported by the Robert A. Welch Foundation, Houston, Texas.

[1] R. J. Cava, B. Batlogg, J. J. Krajewski, R. C. Farrow, L. W. Rupp, A. E. White, K. Short, W. F. Peck, and T. Kometani, Nature **337**, 814 (1988).

[2] R. J. Cava, P. Gammel, B. Batlogg, J. J. Krajewski, W. F. Peck, Jr., L. W. Rupp, Jr., R. Felder, and R. B. van Dover, Phys. Rev. B **42**, 4815 (1990).

[3] L. F. Mattheiss and D. R. Hamann, Phys. Rev. B **26**, 2686 (1982).

[4] G. Larramona, C. Gutierrez, I. Pereira, M. R. Nunes, and F. M. A. da Costa, J. Chem. Soc. Faraday Trans. **85**, 907 (1989).

[5] D. J. Singh, D. A. Papaconstantopoulos, J. P. Julien, and F. Cyrot-Lackmann, Phys. Rev. B **44**, 9519 (1991).

[6] M. G. Smith, J. B. Goodenough, A. Manthiram, R. D. Taylor, W. Peng, and C. W. Kimball, J. Solid State Chem. **98**, 181 (1992).

[7] M. Eibschutz, R. J. Cava, J. J. Krajewski, W. F. Peck, Jr., and

W. M. Reiff, Appl. Phys. Lett. **60**, 830 (1992).
[8]J. J. Yeh and I. Lindau, At. Data Nucl. Data Tables **32**, 1 (1985).
[9]C. D. Wagner, W. M. Riggs, L. E. Davis, J. F. Moulder, and G. E. Muilenberg, *Handbook of X-Ray Photoelectron Spectrosopy* (Perkin-Elmer, Eden Prairie, MN, 1979).
[10]We were not able to determine the band gap of undoped $BaSnO_3$ by combined UPS and BIS, because the sample charged heavily due to its insulating nature.
[11]M. Jansen, Angew. Chem. Int. Ed. **17**, 137 (1978).